An Observational Study of Large-Scale Atmospheric Rossby Waves during FGGE

RICHARD S. LINDZEN

Department of Earth, Atmospheric and Planetary Sciences, Massachusetts Institute of Technology, Cambridge, MA 02139

DAVID M. STRAUS

Goddard Laboratory for Atmospheric Sciences, Global Modeling and Simulation Branch, NASA/Goddard Space Flight Center, Greenbelt, MD 20771

BERT KATZ

M/A-COM Sigma Data Incorporated, Global Modeling and Simulation Branch, NASA/Goddard Space Flight Center, Greenbelt, MD 20771

(Manuscript received 20 September 1983, in final form 28 December 1983)

ABSTRACT

Analyzed global data from the European Centre for Medium Range Weather Forecasts for the FGGE year are projected onto Hough functions at each synoptic time and the time series filtered to retain all westward propagating components on time scales less than seasonal. The evolution of Hough mode phase agrees closely with Rossby wave theory whenever the amplitudes are not small. The evolution of the wave amplitude is described as irregular vacillation. The first three zonal and meridional wavenumbers are studied. The total Rossby wave field can be as large as 130 m and can potentially explain a significant part of observed, persistent anomalies.

1. Introduction

In a rotating spherical atmosphere, in the absence of relative mean winds and damping, there will exist free oscillations or normal modes, described by Laplace's tidal equation. These oscillations fall into two categories: gravity waves modified by rotation and Rossby waves which owe their existence to the variation of the vertical component of the rotation vector with latitude (more precisely to the meridional variation of potential vorticity). The latter were first studied in explicit connection with their potential meteorological significance by Rossby *et al.* (1939). For nondivergent flow on a β-plane, Rossby obtained the well-known dispersion relation for the phase speed of such waves, i.e.,

$$c = U - \frac{\beta}{k^2}, \tag{1}$$

for waves of the form $e^{ik(x-ct)}$, where x is eastward distance, t time, k zonal wavenumber, c eastward phase speed, U mean eastward flow and β the northward gradient of the Coriolis parameter. Although (1) fails to include important effects due to divergence, sphericity and meridional wave structure (all of which are included in current studies viz. Kasahara, 1980; Salby, 1981a,b), it does highlight the following important features: The value of c relative to U is always negative and diminishes in magnitude as the horizontal scale ($\sim k^{-1}$) diminishes. Now U is not, in general, constant (on a sphere, the mean angular velocity is not constant) and when the variation of U becomes comparable to $c - U$ calculated from (1), one intuitively expects critical surfaces to develop and the discrete spectrum to disappear. This has, in fact, been shown by Kasahara (1980) and Salby (1981a, 1981b). However, for very large scales (small k), this does not occur and discrete Rossby waves of the sort discussed should exist, at least in an approximate sense. The study of such waves—both theoretically and observationally—has been conducted fairly extensively since 1940, and a comprehensive review of this work is given by Madden (1979).

For the purposes of the present paper, several earlier results prove especially important:

1) At large planetary scales, westward traveling Rossby waves will coexist with stationary waves forced by geographically stationary distributions of orography and relatively stationary distributions of heating (Haurwitz, 1940), and possibly with eastward traveling baroclinic instabilities (Pratt and Wallace, 1976). The analysis of Rossby waves thus calls for the separation of these waves in the data.

2) Eliasen and Machenhauer (1965) decomposed the height field at 500 mb into spherical harmonics and discovered that the largest scales for wavenumbers

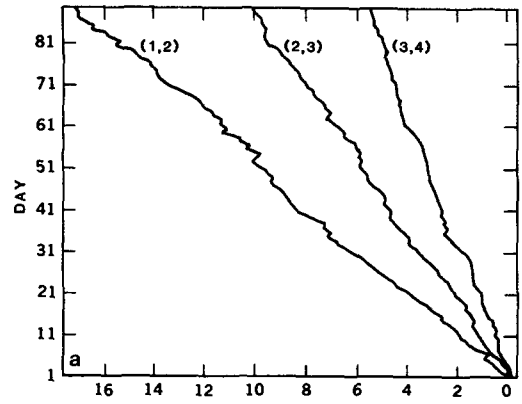

FIG. 1a. Successive daily values of the phase angle for the 24 h tendency field in the streamfunction at the 500 mb level for the spherical harmonic projections (1, 2), (2, 3) and (3, 4) during the 90-day period beginning 1 December 1956. The abscissa shows the number of westward circulations around the earth after the first passage of the Greenwich meridian. (Redrawn from Eliasen and Machenhauer, 1965.)

1, 2 and 3 contained westward traveling components whose phase speeds roughly agreed with estimates based on the spherical counterpart of (1). These results are reproduced in Figs. 1a and 1b.

3) Diky and Golitsyn (1968) showed that when calculations of Rossby waves took account of divergence (for an atmosphere with an equivalent depth of 10 km) and the atmosphere's mean angular velocity, then excellent agreement with Eliasen and Machenhauer's (1965) observed phase speeds was obtained. More recent calculations do not alter these results.

4) Kasahara (1980, 1981) and Ahlquist (1982), in calculating the normal mode eigenfunctions (Hough modes) in the presence of realistic meridional distributions of zonal wind, found that for the largest scales (zonal wavenumbers 1, 2, 3, and the first three or four meridional modes) the wind altered predicted periods but only mildly changed the Hough modes themselves. Salby (1981a,b) computed the three-dimensional normal mode response of the atmosphere in the presence of realistic two-dimensional zonal wind configurations by perturbing the full linearized system of equations with bottom forcing and monitoring the response as a function of the forcing frequency. He found that the spatial structures of the gravest modes were little changed from the no mean wind case in the troposphere, but that the realistic winds caused the modes to have a band of frequencies rather than a single discrete eigenvalue (i.e., spectral lines were broadened). This was especially true of the (2, 4), (2, 5), (3, 4), (3, 5) and (3, 6)[1] modes. Indeed, the relevant peaks in

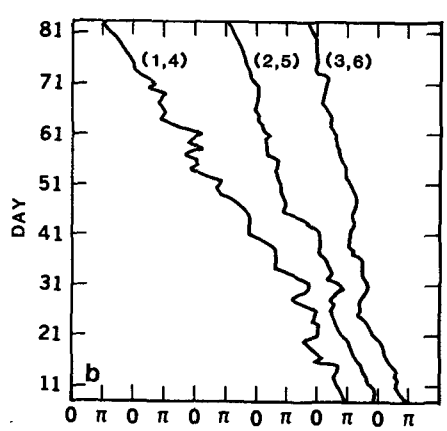

FIG. 1b. Successive daily values of the phase angle (radians) for the deviation of the streamfunction from the 15-day mean field at the 500 mb level for the spherical harmonic components (1, 4), (2, 5) and (3, 6). The days are numbered from 1 December 1956. (Redrawn from Eliasen and Machenhauer, 1965.)

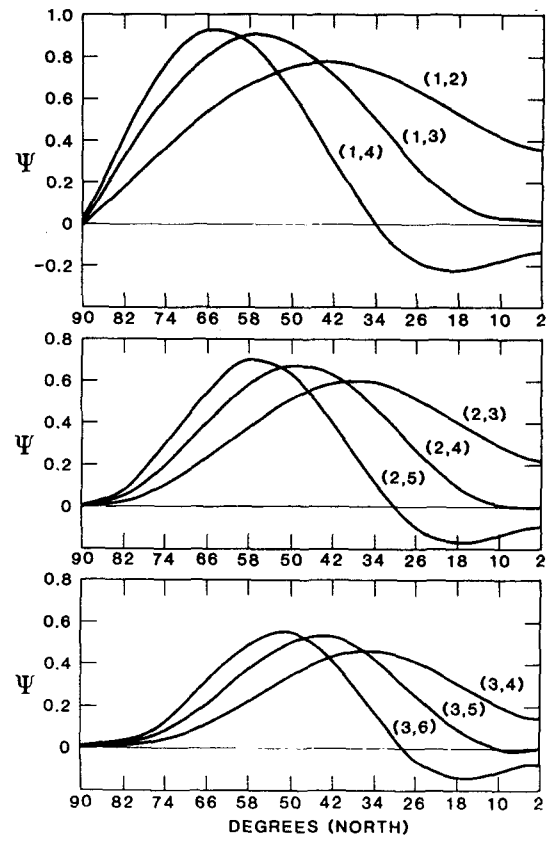

FIG. 2. Dimensionless eigenfunctions necessary to convert wave amplitudes reported in the figures to physical amplitudes for the geopotential height field.

[1] The spherical harmonic indices (s, n) refer to the dominant associated Legendre function for the streamfunction. Noting that the geopotential height field has the opposite symmetry from the streamfunction, $n - s$ = even (odd) then refers to a mode for which the height field is antisymmetric (symmetric) about the equator.

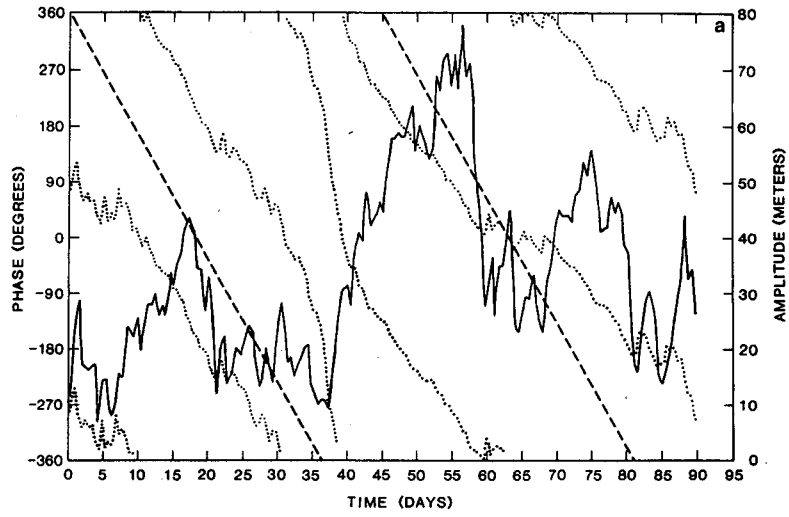

FIG. 3a. Amplitude and phase of (1, 4) Hough mode for December–February as defined by Eq. (2.4) in the text. The amplitude is given by the solid line, with the corresponding scale on the right, while the phase is given by the dotted line, with the corresponding scale on the left. Two cycles of the phase are plotted. The dashed line corresponds to the phase evolution that would occur were the Hough function to propagate uniformly westward with the period given by Table 1.

the spectra of zonal wavenumber perturbations (Madden, 1978) and of Hough modes (Ahlquist, 1982) show bandwidths of about 0.05 to 0.20 cycles per day, although it is not clear whether this broadening is due to the effects of spatial and/or temporal zonal wind variations, frictional decay, wave transiency or vertical leakage. (The last possibility was discussed by Lindzen and Blake, 1972, for acoustic-gravity waves and by Salby, 1980, for Rossby modes.)

5) Madden (1978) showed that for zonal wavenumber 1, westward propagating waves with periods of 5 days and 16 days had the meridional structures of the Hough modes normally expected to have these periods. Other modes were not investigated. Madden and Labitzke (1981) also identified an episode during the winter of FGGE in which the 16-day wave had a very large amplitude.

6) Madden (1978) noted that the vertical structure of Rossby waves closely corresponded to that of Lamb waves (Lindzen, 1967), having slow exponential growth

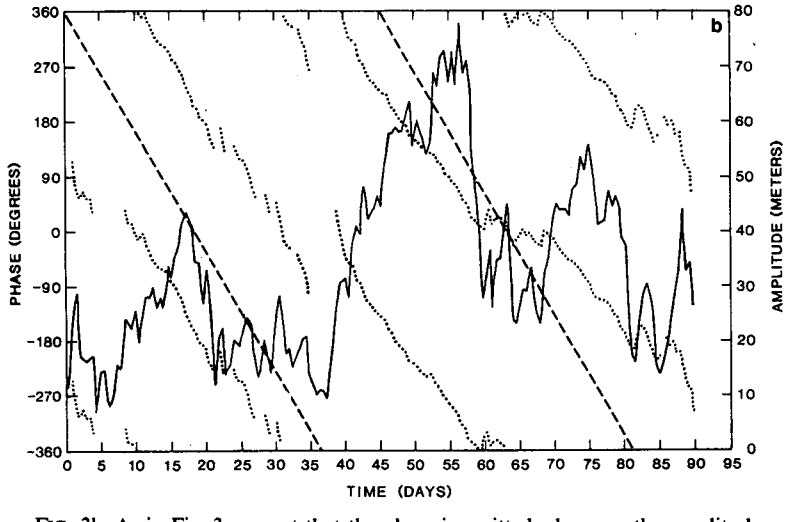

FIG. 3b. As in Fig. 3a except that the phase is omitted whenever the amplitude falls below a certain fraction p of its maximum value. Here $p = 0.20$.

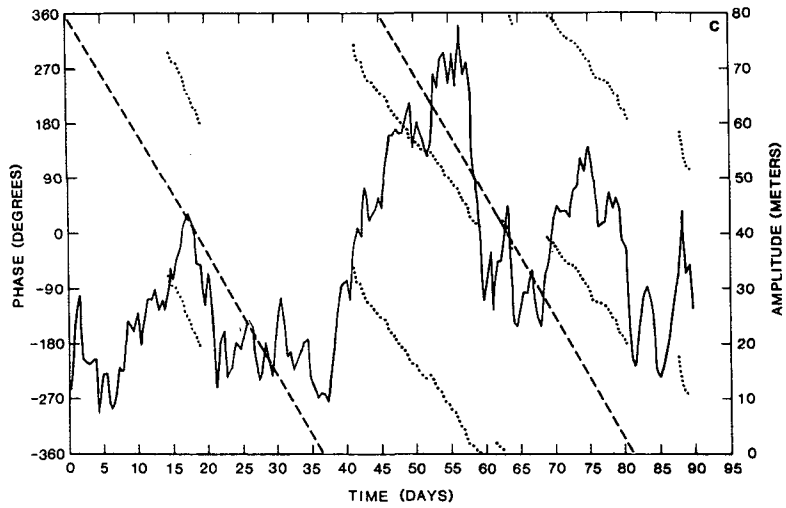

FIG. 3c. As in Fig. 3a, with $p = 0.40$.

with height. Relatedly, Pratt and Wallace (1976) noted that barotropic vertical structures accounted for the bulk of westward moving variance.

Figures 1a and 1b, showing the cumulative phase of spherical harmonic projections, might suggest that Rossby waves could exist as coherent waves over very long periods. If true, this result would be very odd indeed. Ninety days is much longer than frictional spindown times (1–3 weeks) and Rossby waves are not unstable perturbations on the basic flow. What does force free Rossby waves is still an unanswered question, but suggested mechanisms include forcing by stochastic noise (Garcia and Geisler, 1981) and regularly oscillating mean winds (Hirota, 1971). Forcing by irregular variations in the zonal mean winds, while not specifically addressed by the above studies, is another possibility. To assess these various proposals, information on the behavior of Rossby wave amplitudes as a function of time is needed. Unfortunately, Eliasen and Machenhauer (1965) did not present the evolution of wave amplitude that corresponds to the phase progression shown in Figs. 1a and 1b. Kasahara (1976) presented the average standard deviation of Hough mode coefficients for a 24-day period in December of 1972 and found averaged amplitudes of 50–100 m for the 500 mb height field for the lowest few zonal and meridional wavenumbers. Averaged amplitudes of the order of 80 m at 1000 mb were reported by Ahlquist (1982), who based his estimates on spectra obtained from 3¼ years of global analyses at several levels. More relevant to the current study are the papers of Madden (1978) and Madden and Labitzke (1981), who studied the time evolution of the (1, 2) and (2, 4) Rossby modes, but only for limited periods when the waves were particularly strong.

The purpose of this paper is to present a portrait of the evolution of the global-scale Rossby waves discussed above. In contrast to the above studies, emphasis is placed on the temporal evolution of the amplitude and phase of Hough modal projections, rather than on characteristics of the time spectra of these waves. Another important aspect of this study of Rossby waves is our use of data from the first GARP Global Experiment (FGGE). Since these waves are global in extent and depend on the height *and* wind fields for their definition, the use of analyses which do not have adequate coverage in the tropics and over oceanic regions may lead to significant errors in the diagnosis of wave quantities. In this respect, the FGGE level III-b data represent one of the best global gridded datasets available for an extended period of time. We will show that the first three meridional Rossby waves associated with wavenumbers 1–3 are indeed noticeably present at 500 mb throughout the FGGE year, with the amplitudes of the second and third meridional modes being substantial (of order 50 m) much of the time. The portraits

TABLE 1. Rossby wave periods (days) calculated by Kasahara (1980) for climatological mean 500 mb winds.

Mode	Winter	Spring	Summer	Autumn
(1, 2)	4.85	4.87	4.85	4.85
(1, 3)	9.91	9.99	9.49	9.52
(1, 4)	18.39	17.22	16.68	17.40
(2, 3)	3.84	3.84	3.79	3.84
(2, 4)	7.27	7.55	6.93	7.07
(2, 5)	14.23	13.54	12.71	13.22
(3, 4)	4.28	4.22	4.10	4.22
(3, 5)	7.40	7.60	6.73	7.06
(3, 6)	13.65	13.89	11.78	12.76

TABLE 2. Theoretical range of periods (days) from Salby (1981b), denoted by S. Also indicated are the observational periods of Eliasen and Machenhauer (1965), denoted by EM.

	Period			Period			Period	
Mode	S	EM	Mode	S	EM	Mode	S	EM
(1, 2)	3.3–5.6	5	(2, 3)	3.8–4.5	4.5	(3, 4)	4–4.8	6
(1, 3)	9.1–11.1	—	(2, 4)	6.7–7.7	—	(3, 5)	6.7–8.3	—
(1, 4)	14.3–20	8	(2, 5)	11.1–20	15	(3, 6)	11.1–20	15

of phase and amplitude history show a regular westward phase propagation (with nearly the expected period) whenever the amplitudes are relatively large, and irregular phase propagation for small amplitudes. The amplitude evolution takes the form of a series of pulses of duration of about 5–20 days, indicating that the waves have an episodic nature, growing and decaying on time scales not longer than a few wave periods, at most. This behavior is shown to be independent of the analysis–forecast procedure used by a comparison of results between two different analysis schemes. The presence of what is essentially irregular vacillation cautions against the misuse of band-pass filtering; too narrow a band-pass filter would distort the evolution of these waves. Accordingly, our analysis procedure (see below) incorporates a minimum of filtering.

The analysis of the data was strongly guided by the considerations given in the opening paragraphs. As a result of point 6, we felt it was adequate to consider the 500 mb level in isolation from the others, while point 4 indicated that the Hough functions were good approximations to the "true" eigenfunctions. Thus, the first steps of the analysis consisted of projecting the 500 mb height and wind data onto Hough functions for each synoptic time. Following the cautions given above against excessive filtering, we then filtered the data *minimally* by removing the seasonal cycle and eastward propagating components on a seasonal basis; *all* westward propagating components not removed as part of the seasonal cycle were retained. Complete details of the data analysis are given in Section 2. The amplitude and phase histories for all four seasons of the FGGE year are discussed in Section 3, the relevance of the waves for observed meteorological flows is described in Section 4, while Section 5 compares results from two different analysis schemes and Section 6 contains concluding remarks.

2. Data and methods

The data used were the level III-b gridded data for FGGE, as prepared by the European Centre for Medium Range Weather Forecasts (Bengtsson *et al.*, 1982), hereafter referred to as ECMWF. The time period covered is 1 December 1978–30 November 1979, twice per day, at 0000 GMT and 1200 GMT. (The data are available more often during the two Special Observing Periods; however, these additional data were not used.) This dataset was obtained from the National Meteorological Center in the standard FGGE format, and the data were unpacked and interpolated from the

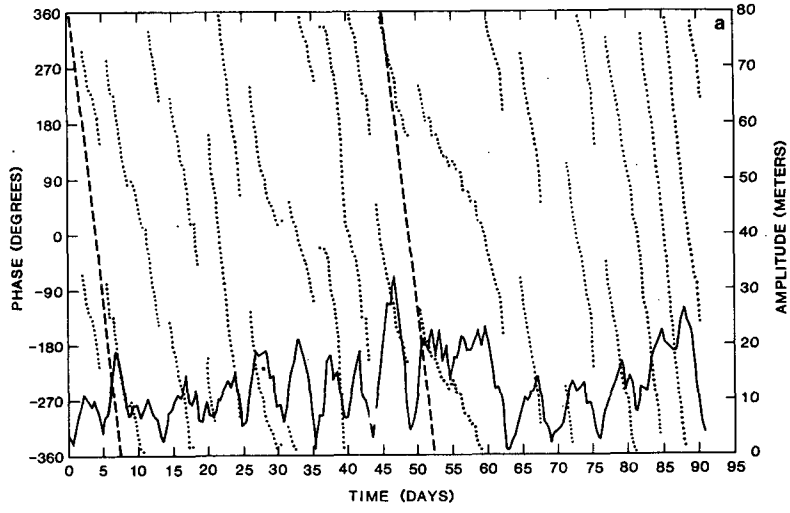

FIG. 4a. Amplitude and phase of the (2, 3) Hough mode for September–November. As in Fig. 3a, with $p = 0.20$.

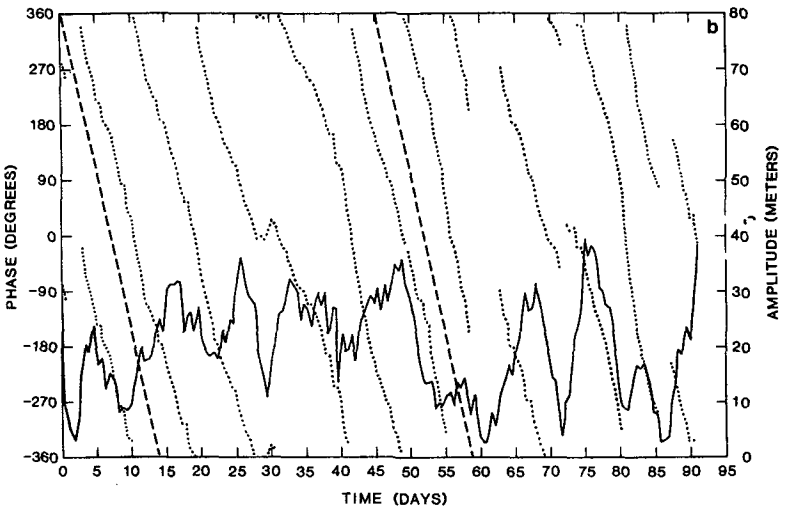

FIG. 4b. Amplitude and phase of the (2, 4) Hough mode for September–November. As in Fig. 3a, with $p = 0.20$.

original 1.875° × 1.875° latitude–longitude grid to a 4° × 5° latitude–longitude grid using a 16-point Bessel interpolation method. Only the 500 mb geopotential height field (z) and horizontal wind fields (u, v) were used.

From this point on, the data are handled on a seasonal basis, with Northern Hemisphere winter comprising the months of December, January and February (winter); March, April and May (spring); June, July and August (summer); and September, October and November, (autumn). As previously mentioned, the fields of z, u and v were projected onto Hough functions for each synoptic time for each season. The calculations of the Hough functions used an equivalent depth of 10 km and were carried out by the use of a shooting method (see Katz, 1982). The Hough functions considered are those given by $(s, n) = (1, 2), (1, 3), (1, 4), (2, 3), (2, 4), (2, 5), (3, 4), (3, 5)$ and $(3, 6)$.

The projection onto the Hough functions follows the procedure described by Kasahara (1976), so that the fields u, v and $h = gz$ are written (for a single zonal wavenumber s) as:

$$\begin{bmatrix} u(\lambda, \mu) \\ v(\lambda, \mu) \\ h(\lambda, \mu) \end{bmatrix} = \sum_{n \geq s} \begin{bmatrix} U_n^s(\mu)[a_n^s \cos(s\lambda) + b_n^s \sin(s\lambda)] \\ V_n^s(\mu)[a_n^s \sin(s\lambda) - b_n^s \cos(s\lambda)] \\ c\Psi_n^s(\mu)[a_n^s \cos(s\lambda) + b_n^s \sin(s\lambda)] \end{bmatrix}. \quad (2.1)$$

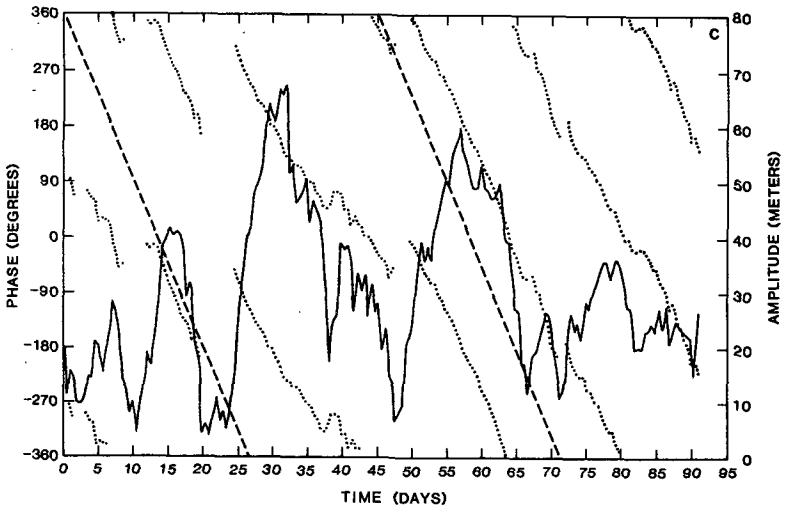

FIG. 4c. Amplitude and phase of the (2, 5) Hough mode for September–November. As in Fig. 3a, with $p = 0.20$.

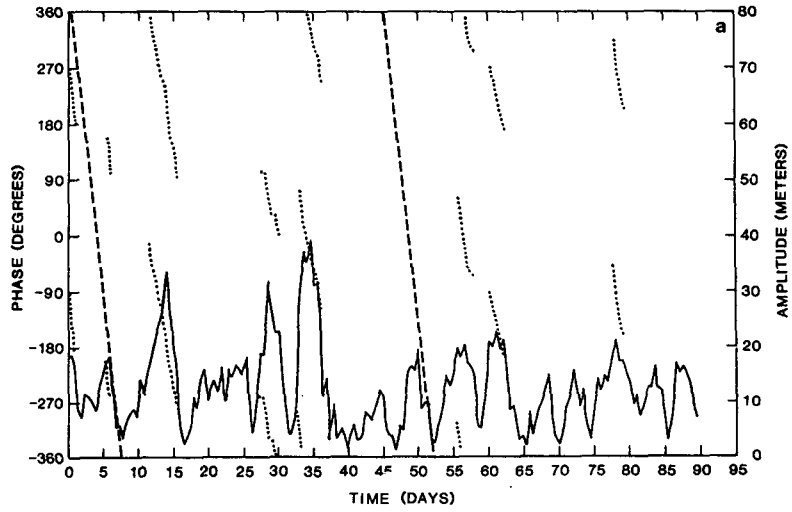

FIG. 5a. Amplitude and phase of the (2, 3) Hough mode for December–November. As in Fig. 3a, with $p = 0.40$.

Here λ is longitude, μ = sine (latitude), and $c = (gH)^{1/2}$, with g the gravitational acceleration and H the equivalent depth. The functions $U_n^s(\mu)$, $V_n^s(\mu)$ and $\Psi_n^s(\mu)$ are dimensionless and satisfy

$$\frac{1}{2}\int_{-1}^{1} d\mu[U_n^s(\mu)U_{n'}^s(\mu) + V_n^s(\mu)V_{n'}^s(\mu) + \Psi_n^s(\mu)\Psi_{n'}^s(\mu)] = \delta_{n,n'}. \quad (2.2)$$

The coefficients a_n^s and b_n^s have dimensions of m s^{-1}. From (2.1), $z(\lambda, \mu)$ can be expressed, for a given Hough mode, as

$$z(\lambda, \mu) = \frac{c}{g}\Psi_n^s(\mu)[a_n^s \cos(s\lambda) + b_n^s \sin(s\lambda)], \quad (2.3)$$

where c/g has the numerical value of 31.94 s.

At this point, then, the data to be analyzed take the form of seasonal time series of a_n^s nd b_n^s for each mode (s, n). Each of these time series was detrended by removing a parabolic seasonal cycle, following Straus (1983). In order to filter out the eastward propagating portions of the wave fields given in (2.1) or (2.3), the series a_n^s and b_n^s were Fourier transformed in time. The westward propagating contribution to the Fourier transforms were computed (Hayashi 1971; Straus and Shukla, 1981) and from these the time series were resynthesized. This method insures that all westward propagating components not contributing to the seasonal cycle were kept, regardless of frequency. (Since the component of the field at the Nyquist frequency

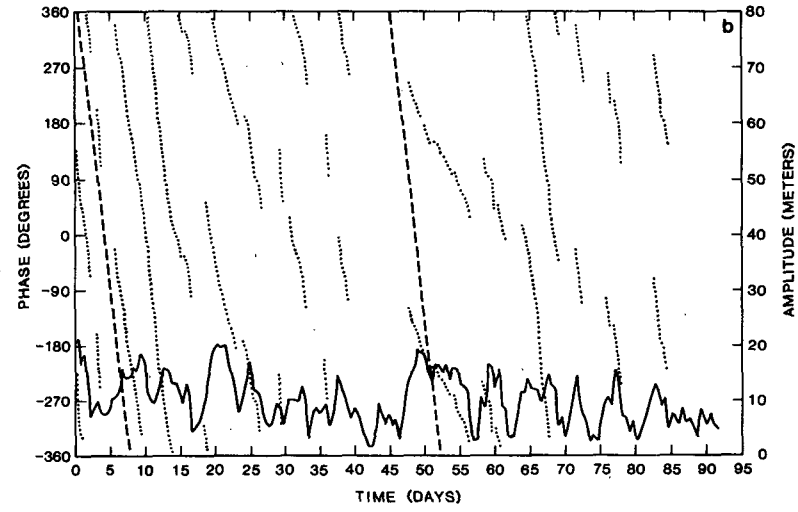

FIG. 5b. Amplitude and phase of the (2, 3) Hough mode for March–May. As in Fig. 3a, with $p = 0.40$.

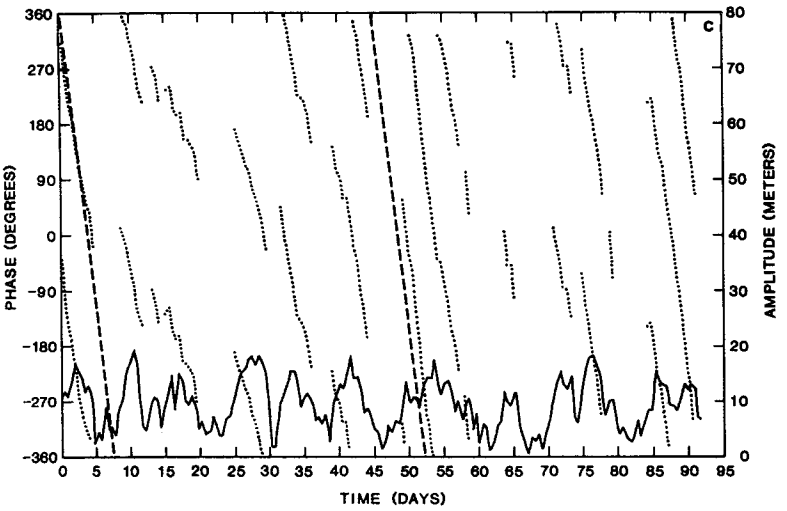

FIG. 5c. Amplitude and phase of the (2, 3) Hough mode for June–August. As in Fig. 3a, with $p = 0.40$.

of 1 cycle per day cannot be uniquely decomposed into westward and eastward propagating parts, the entire Nyquist component was retained.) Note that to the extent that true standing oscillations (i.e., oscillations fixed in space) are present, this analysis retains only the westward propagating components of such oscillations. The results do not indicate that this is a major limitation in our procedure.

From the resynthesized time series a_n^s and b_n^s, series of amplitude A and phase ϕ were computed, where A and ϕ are defined from

$$z(\lambda, \mu) = \frac{c}{g} \Psi_n^s(\mu)\{a_n^s \cos(s\lambda) + b_n^s \sin(s\lambda)\} = \Psi_n^s(\mu) A \cos(s\lambda - \phi). \quad (2.4)$$

The range of the phase is thus $-\pi$ to π, independent of wavenumber s. It is important to note that in order to get the amplitude of the wave pattern for the physical z field at any latitude, one must multiply A by the dimensionless function Ψ_n^s, for the appropriate mode. These functions are presented in Fig. 2 for the Northern Hemisphere. [The functions for modes (1, 2), (2, 3) and (3, 4) are actually the negative of those shown in Fig. 2.] To obtain the behavior in the Southern Hemisphere, note that the functions for modes (1, 2), (1, 4), (2, 3), (2, 5), (3, 4) and (3, 6) are even with respect to the equator while those for (1, 3), (2, 4) and (3, 5) are odd. It is apparent that the maximum value of Ψ_n^s ranges from near 1.0 for the (1, 3) and (1, 4) modes to about 0.4 for the (3, 4) mode. A given am-

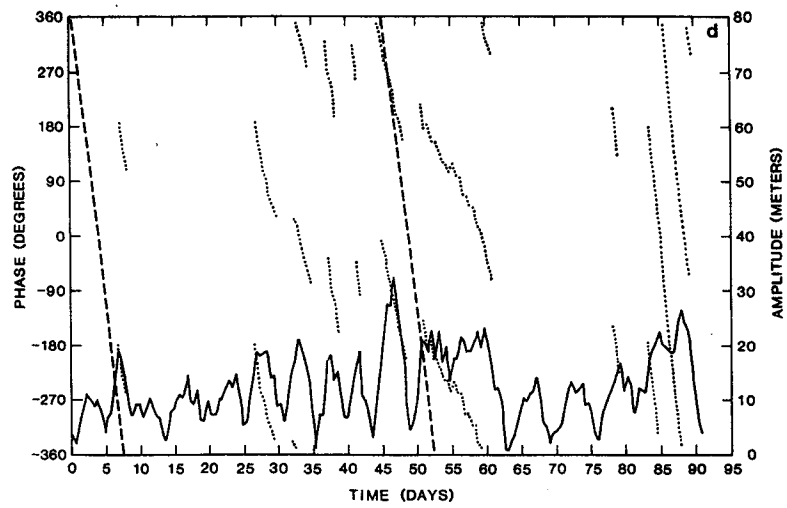

FIG. 5d. Amplitude and phase of the (2, 3) Hough mode for September–November. As in Fig. 3a, with $p = 0.40$.

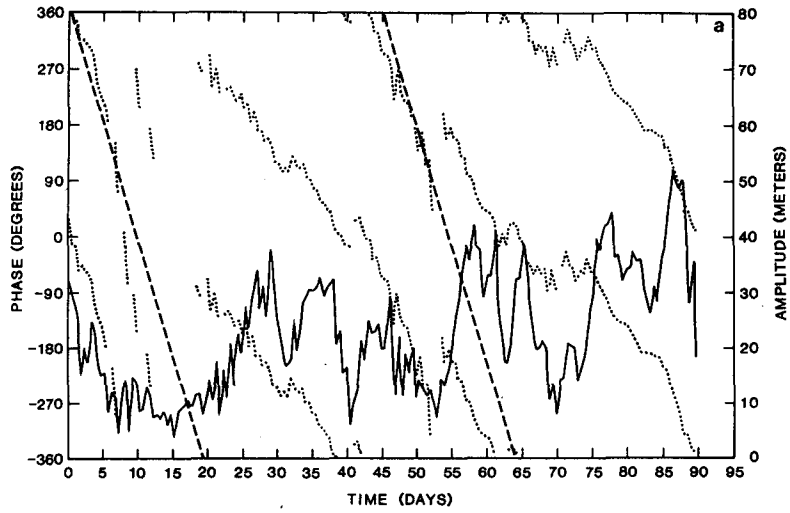

FIG. 6a. Amplitude and phase of the (1, 3) Hough mode for December–February. As in Fig. 3a, with $p = 0.20$.

plitude A thus translates into a physical amplitude which for the former modes is about 2½ times that for the latter mode.

3. Rossby wave amplitudes and phases

The amplitude and phase histories of the winter (1, 4) mode are portrayed in Figs. 3a–c. This mode is used to illustrate several features which all the modes have in common. The "irregular vacillation" referred to in the Introduction is apparent as a sequence of pulses in the amplitude. Especially noticeable are the episodes of large amplitude taking place from days 42 to 59 (10–28 January) and from days 72 to 79 (10–17 February. At 66°N [the latitude corresponding to the maximum of the (1, 4) Hough mode, as in Fig. 2], the wave amplitudes attained peak values of about 70 and 50 m, respectively.

The phase[2] history of the (1, 4) mode presented in Fig. 3a shows a tendency for wastward propagation with a wave period near that calculated theoretically by Kasahara (1980). Kasahara's periods (valid for climatological seasonal mean winds) are given in Table 1. On each phase plot, the straight line phase progression corresponding to the appropriate theoretical period is indicated by dotted lines in Fig. 3. To be sure, the real atmosphere does not sustain modes with a single, perfectly defined phase speed; rather we should expect a range of phase speeds. The width of this range was determined by Salby (1981b) for steady, spatially varying mean winds in a baroclinic atmosphere and is indicated for each mode in Table 2. Moreover, additional variability in period can arise from the temporal variability of the zonal wind. The phase history in Fig. 3a shows episodes when the wave's phase speed is drastically different from the theoretical prediction and lies outside the range indicated in Table 2, such as on days 36–38. The strong impression received from from Fig. 3a (and similar plots for the other modes) is that such episodes usually occur when the wave amplitude is a minimum. To test this notion, we examined the wave evolution, defining the phase only when the amplitude was above some cutoff fraction p of its maximum value for the season. The results for a cutoff of $p = 0.20$ (Fig. 3b) and $p = 0.40$ (Fig. 3c) confirm that when the episodes of small amplitude are eliminated, the phase progresses westward with a phase speed remarkably close to the predicted Rossby phase speed. Stated differently, Figs. 3a–c roughly defined a noise level (amplitude 40% of the maximum) above which the Hough mode propagates as a Rossby wave.

For other modes, the slope of the phase history lines does not always agree with the theoretical slope given by the barotropic theory, but it usually lies within the range indicated by baroclinic theory (Table 2). Occasionally, the phase speed does not lie within this range. However, in a given set of modes for the same wavenumber [e.g., (1, 2), (1, 3), (1, 4)], the phase speed of each mode, variable as it is, is still noticeably different from the phase speed of the neighboring mode. This is illustrated in Figs. 4a–c for the autumn (2, 3), (2, 4) and (2, 5) modes. With a cutoff criterion of $p = 0.20$, there are instances during the evolution of both the (2, 3) and (2, 4) phase when the phase moves

[2] The phase is plotted from -2π to $+2\pi$, thus giving two phases, separated by 2π, at each instant in time. Such a "double" phase plot makes the phase progression quite clear visually. The presence of episodes in which the total wave moves eastward can be expected on occasion, even though each Fourier component moves westward (Ahlquist, personal communication, 1983).

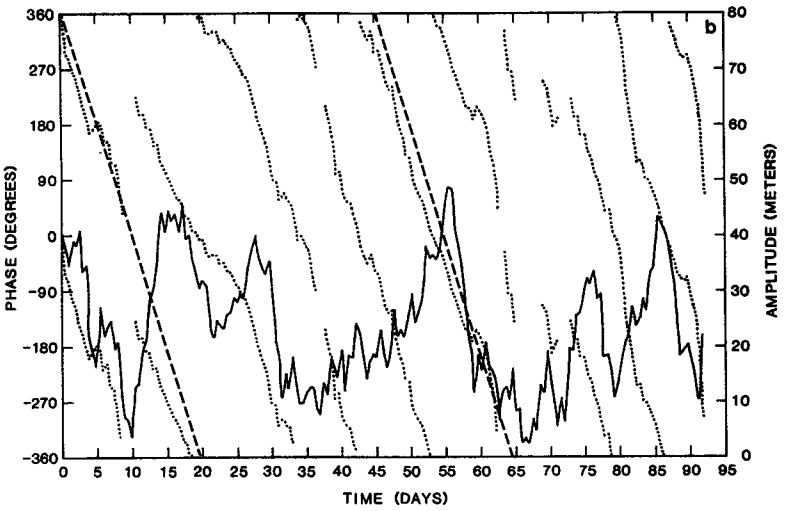

FIG. 6b. Amplitude and phase of the (1, 3) Hough mode for March–May. As in Fig. 3a, with $p = 0.20$.

irregularly or with the "wrong" phase speed. Yet, on the whole, the wave period of each mode is well defined and is distinct from that of the other two modes.

The amplitude histories portrayed in Figs. 4a–c show several characteristics which are typical of all the modes examined. As the meridional index increases, the amplitudes become larger and the time scale for their change generally increases. The increase of amplitude within meridional index was obtained theoretically by Salby (1980), who attributed it to the larger effective forcing felt by the higher modes, due to their longer periods. In addition, topography does not contribute much forcing to the gravest modes. The fluctuations of large amplitude for the (2, 3) mode have characteristic widths of 5–10 days (about 1.5–2.5 wave periods), whereas the pulse widths for the higher [(2, 4) and (2, 5)] modes are about 10–20 days. These numbers are generally applicable to all the modes. It is clear that while episodes of well-defined wave propagation generally last for at least one-half a wave period, they rarely, if ever, endure for more than three wave periods.

It is of some interest to determine whether the behavior of these global waves exhibits a large seasonal dependence. Figs. 5, 6 and 7 address this question by portraying the evolution of the (2, 3) mode, the (1, 3) mode and the (3, 6) mode for the four seasons. These modes were chosen as examples of 4–5 day modes, 7–10 day modes and 14–18 day modes, respectively

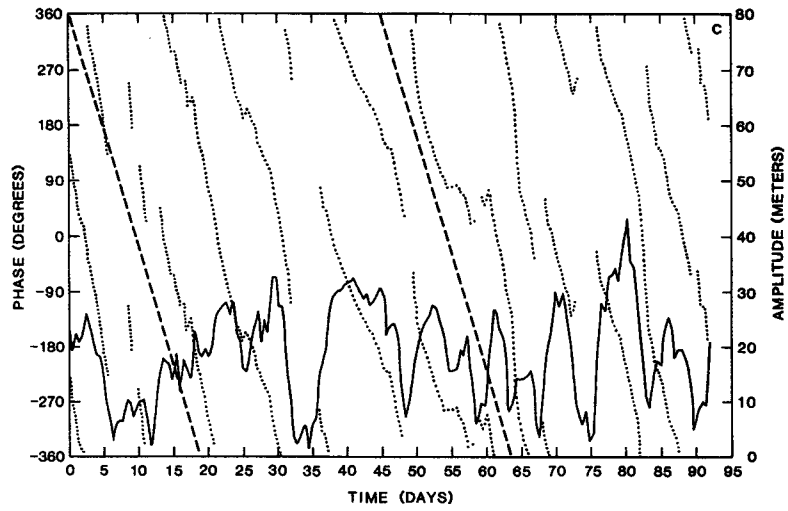

FIG. 6c. Amplitude and phase of the (1, 3) Hough mode for June–August. As in Fig. 3a, with $p = 0.20$.

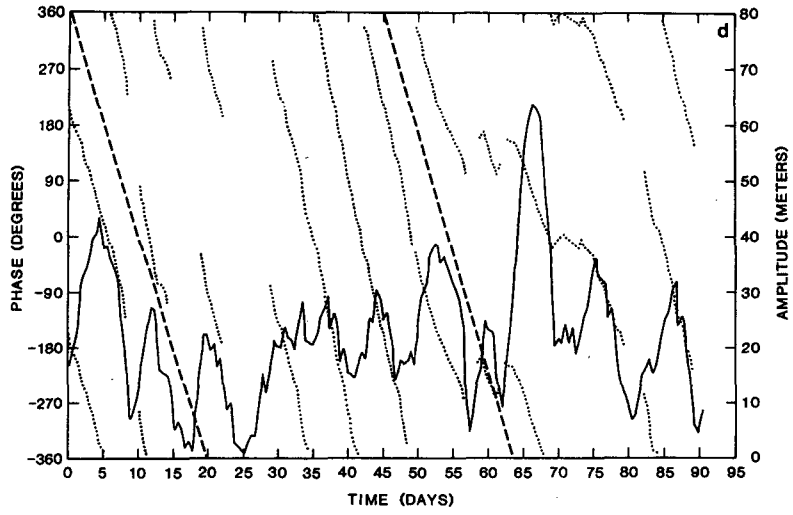

FIG. 6d. Amplitude and phase of the (1, 3) Hough mode for September–November. As in Fig. 3a, with $p = 0.20$.

(see Table 1). These figures show no clear seasonal dependence, but rather, indicate statistical homogeneity with respect to the time of year. The value of the maximum amplitude during the year of each mode (at the latitude where the mode is largest) is given in Table 3, along with the (Northern Hemisphere) season(s) in which this value is attained. The distribution of seasons favors summer and winter over spring and fall, but no one season dominates.

The (2, 3) mode has an amplitude which, on the average, is substantially less than the other two modes. This is generally true; the 4–5 day modes are the weakest of those we have examined (see Table 3). The reader is reminded that the physical amplitudes of the height field z are obtained only after multiplying the plotted amplitudes by the appropriate function from Fig. 2. Although the phase tendencies are generally close to that predicted by theoretical calculations, there are, as before, periods when the observed phase is quite different than predicted [e.g. days 25–40 in winter for the (1, 3) mode] or when the phase speed itself seems to vary in time [e.g., mode (3, 6) during fall].

Although modes of the same meridional wavenumber behave similarly in a statistical sense, it is of interest to determine whether individual pairs of modes are closely connected in the details of their time evolution. One pair that shows such a close connection consists of the (1, 4) winter mode (Fig. 3c) and the (3, 6) winter

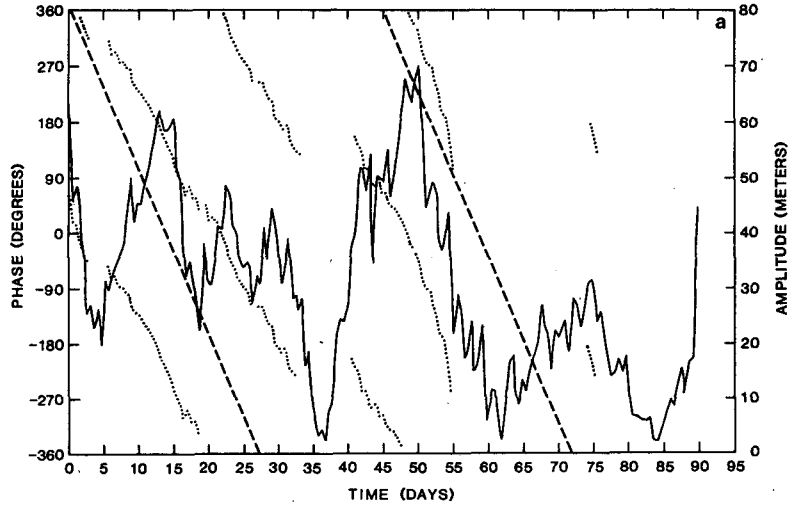

FIG. 7a. Amplitude and phase of the (3, 6) Hough mode for December–February. As in Fig. 3a, with $p = 0.40$.

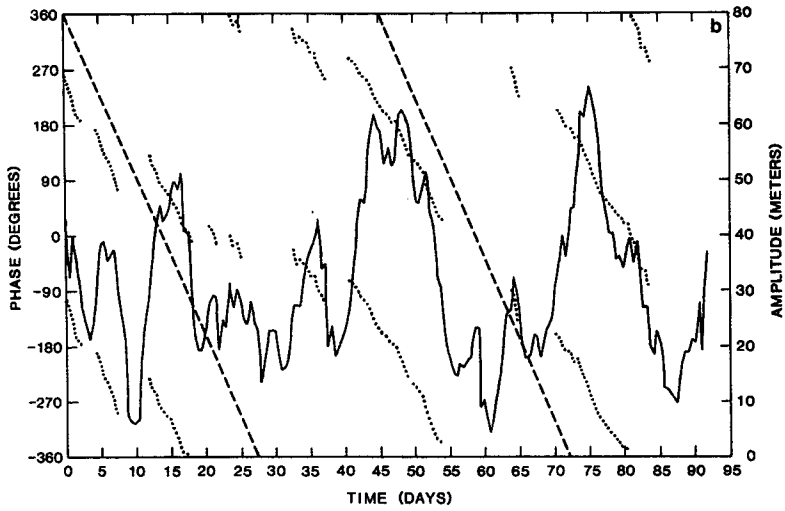

FIG. 7b. Amplitude and phase of the (3, 6) Hough mode for March–May. As in Fig. 3a, with $p = 0.40$.

mode (Fig. 7a). A large surge in mode strength during January occurs for both modes coinciding with the episode discussed by Madden and Labitzke (1981). There are also minima near days 5, 36, 62 and 84 for both modes. Another close correspondence occurs beween winter mode (1, 4) (Fig. 3b) and winter mode (1, 3) (Fig. 6a). As pointed out to the authors by Dr. R. A. Madden, the phases of the two modes track quite well for days 20–40, with the (1, 4) mode leading by 90°. Note that this is precisely the above-mentioned period of time when the (1, 3) mode has the "wrong" phase speed. Some form of mode coupling appears to be in evidence.

4. Total Rossby wave field

The purpose of the present section is to briefly examine the total field contributed by the Rossby waves, at any instant, and to comment on its relationship to the synoptic field at the same instant. Fig. 8a shows the geopotential field at 500 mb obtained by summing the westward propagating components of all nine modes considered for 1200 GMT of 12 January 1979. This date is in the middle of the period during which the (1, 4) and (3, 6) modes reached a large amplitude, as mentioned earlier, and was picked as an example of a period of active Rossby waves. The high center

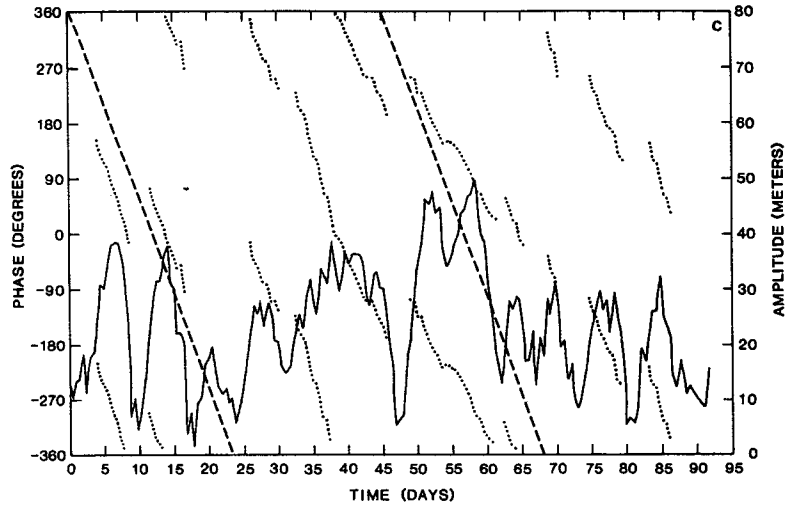

FIG. 7c. Amplitude and phase of the (3, 6) Hough mode for June–August. As in Fig. 3a, with $p = 0.40$.

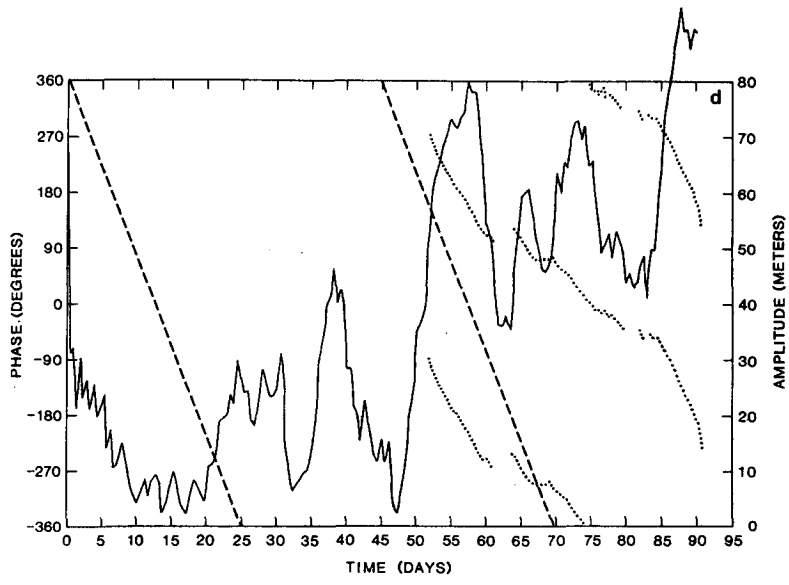

FIG. 7d. Amplitude and phase of the (3, 6) Hough mode for September–November. As in Fig. 3a, with $p = 0.40$.

of 131 m at 65°N, 85°E can be followed as far back as 0000 GMT 9 January, when it was located at 65°N, 125°E and had an amplitude of 78 m, and can be followed as far forward as 1200 GMT 19 January, when it is located at 65°N, 30°E and has an amplitude of 120 m. Of course, during this period, the total wave field changes its shape considerably, consistent with the dispersion of the individual modes.

The total time span for which the wave height field remains above 100 m at 65°N, 85°E is about 3½ days. Although this is not long enough to meet the usual criteria for persistent anomalies (Dole and Gordon, 1983), it clearly suggests that slowly propagating Rossby waves can contribute to such a persistent anomaly.

The total height field of 0000 GMT 12 January is shown in Fig. 8b. The high pressure center at 57°N, 60°E is present for much of the period in question in that general area, although it moves around and is deformed a good deal. The high center in the total Rossby wave field (Fig. 8a) moves into near coincidence with the synoptic high in Fig. 8b toward the end of the period. Thus, the wave may explain the persistence of this feature, but it cannot explain its existence. In fact, the Rossby waves in this case, and in a number of other cases studied by the authors, seem to move quasi-independently of observed synoptic features, sometimes reinforcing them yet tending to counteract them at other times. This does not mean, however, that the Rossby waves have no influence in weather. It is quite possible, for example, that the (short-lived) enhancement of a low-pressure system by the wave field will be just enough to make possible precipitation that would otherwise not occur. In addition, in assessing numerical forecasts, root-mean-square errors in height fields are one common measure of error and the relevance of Rossby waves here is unquestionable. To indicate the range of the total Rossby wave field in the data, we present in Fig. 8c an example of a fairly weak wave field, taken at 1200 GMT 22 October 1979.

TABLE 3. Maximum amplitude and season of Rossby modes. Amplitudes must be multiplied by eigenfunctions of Fig. 2 to obtain physical amplitudes of geopotential height. Seasons refer to the Northern Hemisphere.

Mode	Maximum amplitude (m)	Season(s) in which maximum was reached
(1, 2)	34	summer
(1, 3)	65	autumn
(1, 4)	76	winter
(2, 3)	40	winter
(2, 4)	65	winter
(2, 5)	74	spring, summer
(3, 4)	46	summer, autumn
(3, 5)	60	summer
(3, 6)	90	winter

5. Comparison of different analysis schemes

A very natural and important question is whether the behavior of the Hough mode projections in the ECMWF analyses is characteristic of the real atmosphere, or whether it is an artifact of the particular analysis–forecast scheme used by the ECMWF. In order to resolve this question, we have compared the results

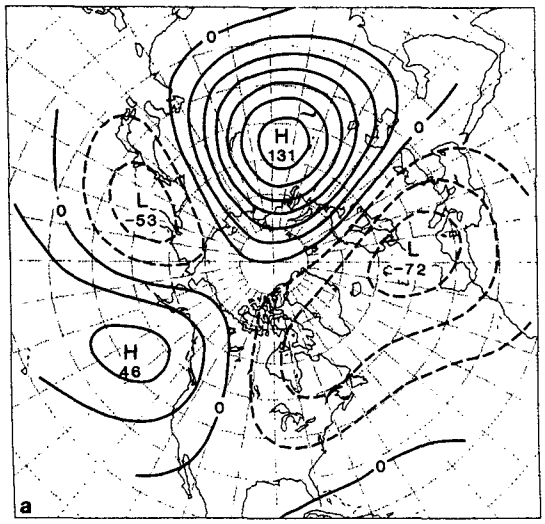

FIG. 8a. Geopotential height field consisting of the sum of all nine westward propagating Hough modes at 500 mb for 1200 GMT 12 January 1979. Contour interval is 20 m.

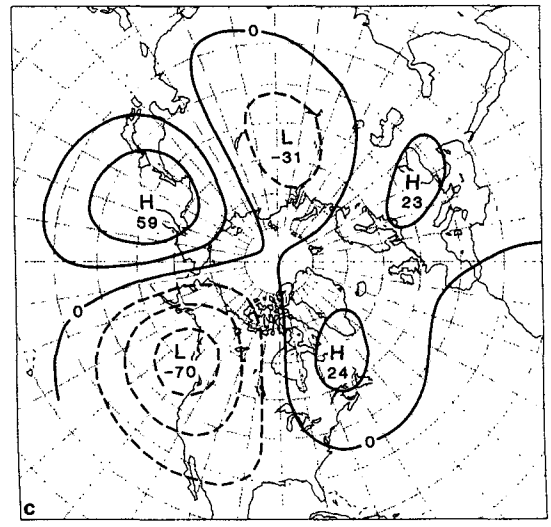

FIG. 8c. Geopotential height field consisting of the sum of all nine westward propagating Hough modes at 500 mb for 1200 GMT 22 October 1979. Contour interval is 20 m.

obtained from the ECMWF analyses with those obtained from the FGGE analyses generated at the Goddard Laboratory for Atmospheric Sciences (GLAS) for the period of 1 May–31 July 1979, twice daily. The GLAS analysis–forecast scheme (documented in Baker *et al.*, 1981) is quite distinct from that of the ECMWF, both in the analysis of observations and in the forecast model used. In particular, normal mode initialization is not employed in the GLAS scheme as it is in the ECMWF scheme.

Both sets of data were processed as a season in the manner described in Section 2, i.e., the seasonal cycle and eastward propagating waves were removed. Figs. 9a and 9b compare the resulting behavior of the amplitude and phase of the (3, 4) mode in the two analysis schemes. All the major peaks and dips of the amplitude evolution match very well between the two figures, while every phase line segment that is portrayed in Fig. 9a (the ECMWF analysis) is also present in Fig. 9b (the GLAS analysis). [The appearance of several phase segments in the GLAS results not present in the ECMWF results arises from the fact that, in both cases, phase was not plotted when the amplitude fell below 20% of its maximum. The inherently noisier behavior of the GLAS analysis scheme (Baker, personal communication, 1983) led to several cases of the amplitude being above the cutoff for the GLAS scheme but not for the ECMWF scheme, so that phase was plotted for the former but not the latter.]

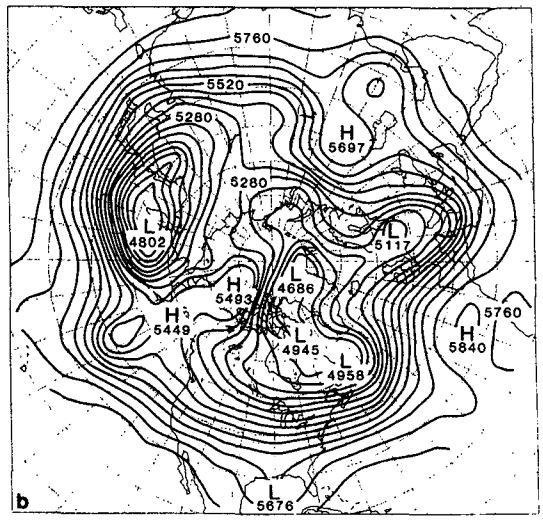

FIG. 8b. Total 500 mb geopotential height field for 1200 GMT 12 January 1979. Contour interval is 60 m.

Close agreement in terms of both amplitude and phase was evidenced in a total of seven out of the nine modes examined. In fact, the agreement is even more striking for some of the other modes, particularly the (2, 5) mode (not shown). The (3, 4) was chosen for graphical presentation because it was "typical" of the seven modes. The comparison between the GLAS and ECMWF results for the (1, 2) and (2, 3) modes showed somewhat less agreement. The amplitudes for both these modes tended to be quite small (order 10 m).

In summary, there is no evidence to support the notion that the Rossby wave-like behavior of the Hough modes is introduced artificially by the analysis–forecast cycle. This behavior seems to be truly characteristic of the atmosphere.

6. Conclusions

A number of properties of observed Rossby waves have been presented in this paper with the hope that

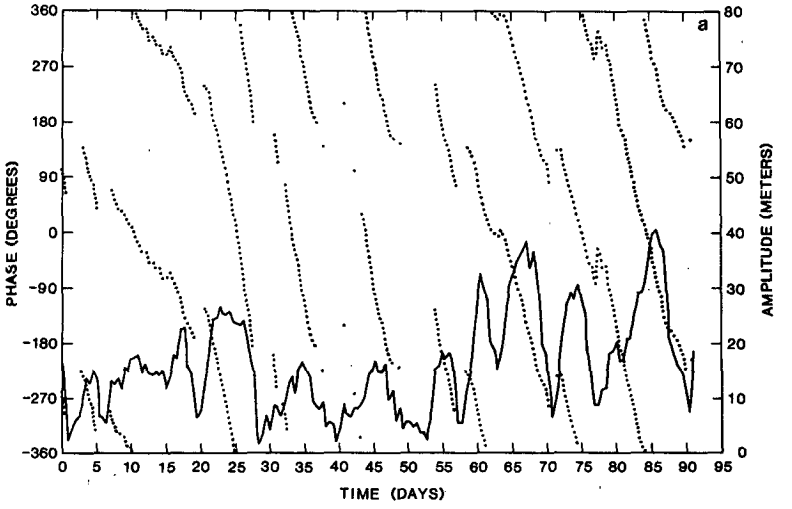

FIG. 9a. Amplitude and phase of the (3, 4) Hough mode for May–July from the ECMWF analyses. The amplitude is given by the solid line, with the corresponding scale on the right, while the phase is given by the dotted lines, with the corresponding scale on the left. Two cycles of the phase are plotted.

it will spur theoretical work regarding the origin of these waves. The most significant conclusion is that, for the largest scales, global Rossby waves exist, i.e., the westward propagating components of Hough modes move relatively uniformly with phase speed in the predicted range when the amplitude is not small. The fact that both symmetric and antisymmetric modes appear equally vigorous implies that a global domain is needed to correctly analyze and/or forecast these waves. The amplitudes undergo an irregular vacillation cycle, which, in general, contains components with time scales longer than the wave period. The seasonal dependence of the wave activity is not marked, but the total wave field can reach an amplitude (for geopotential height) of 130 m at 500 mb, large enough to cause serious errors in analyzed or forecast fields if these waves are not correctly handled by a model (Lambert and Merilees, 1978; Somerville, 1980; Daley *et al.*, 1981; Roads and Somerville, 1982). Note that this amplitude is comparable to that of the stationary waves for the Northern Hemisphere. With regard to synoptic events, the wave field seems to move through individual features in the total field, modifying them but (in general) not drastically so. However, the total Rossby wave field can potentially contribute substantially to persistent anomalies. Whether this contribution is realized in nature remains to be established.

Lastly, we have addressed the question of whether

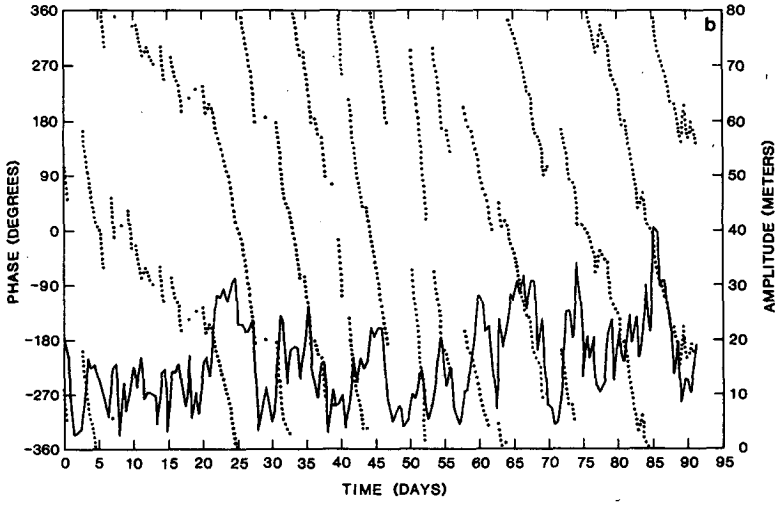

FIG. 9b. As in Fig. 9a but for the GLAS analyses.

the Rossby waves we have documented are an artifact of the ECMWF analysis scheme or whether they occur in nature. Comparisons between ECMWF and GLAS analyses strongly suggest the Rossby waves studied are characteristic of the atmosphere.

Acknowledgments. This work was supported in part by NASA Grant NGL 22 007 228 and by NSF Grant ATM 82 056 38. The authors wish to thank Drs. M. Halem, E. Kalnay, J. Shukla and J. Tenenbaum for many fruitful discussions, Dr. G. DiMego of the National Meteorological Center for providing the data, and the anonymous referees for their suggestions. Special thanks go to Ms. Debbie Sabatino and Ms. Mary Ann Wells for typing the manuscript.

REFERENCES

Ahlquist, J. E., 1982: Normal-mode global Rossby waves: Theory and observations. *J. Atmos. Sci.*, **39,** 193–202.

Baker, S., D. Edelmann, M. Iredell, D. Han and S. Jakkempudi, 1981: Objective analysis of observational data from the FGGE observing systems. NASA Tech. Memo. No. 82062, 132 pp.

Bengtsson, L., M. Kanamitsu, P. Kållberg and S. Uppala, 1982: FGGE 4-dimensional data assimilation at ECMWF. *Bull. Amer. Meteor. Soc.*, **63,** 29–43.

Daley, R., J. Tribbia and D. L. Williamson, 1981: The excitation of large-scale free Rossby waves in numerical weather prediction. *Mon. Wea. Rev.*, **109,** 1836–1861.

Diky, L. A., and G. S. Golitsyn, 1968: Calculation of the Rossby wave velocities in the Earth's atmospherre. *Tellus,* **20,** 314–317.

Dole, R. M., and N. D. Gordon, 1983: Persistent anomalies of the extratropical Northern Hemisphere wintertime circulation: Geographical distribution and regional persistence characteristics. *Mon. Wea. Rev.*, **111,** 1567–1586.

Eliasen, E., and B. Machenhauer, 1965: A study of the fluctuations of the atmospheric planetary flow patterns represented by spherical harmonics. *Tellus,* **17,** 220–238.

Garcia, R. G., and J. E. Geisler, 1981: Stochastic forcing of small-amplitude oscillations in the atmosphere. *J. Atmos. Sci.*, **38,** 2187–2197.

Haurwitz, B., 1940: The motion of atmospheric disturbances. *J. Mar. Res.*, **3,** 35–50.

Hayashi, Y., 1971: A generalized method of resolving disturbances into progressive and retrogressive waves by space Fourier and time cross-spectral analysis. *J. Meteor. Soc. Japan,* **49,** 125–178.

Hirota, I., 1971: Excitation of planetary Rossby waves in the winter stratosphere by periodic forcing. *J. Meteor. Soc. Japan,* **49,** 439–448.

Kasahara, A., 1976: Normal modes of ultralong waves in the atmosphere. *Mon. Wea. Rev.*, **104,** 669–690.

——, 1980: Effect of zonal flows on the free oscillations of a barotropic atmosphere. *J. Atmos. Sci.*, **37,** 917–929.

——, 1981: Corrigendum. *J. Atmos. Sci.*, **38,** 2284–2285.

Katz, B., 1982: Normal modes of primitive equations of atmospheric motion. M.S. thesis, Department of Meteorology, University of Maryland, 110 pp.

Lambert, S. J., and P. E. Merilees, 1978: A study of planetary wave errors in a spectral numerical weather prediction model. *Atmos. Ocean,* **16,** 197–211.

Lindzen, R. S., 1967: Planetary waves on beta planes. *Mon. Wea. Rev.*, **95,** 441–451.

——, and D. Blake, 1972: Lamb waves in the presence of realistic distributions of temperature and dissipation. *J. Geophys. Res.*, **77,** 2166–2176.

Madden, R. A., 1975: Oscillations in the winter stratosphere: Part 2. The role of horizontal eddy heat transport and the interaction of transient and stationary planetary-scale waves. *Mon. Wea. Rev.*, **103,** 717–729.

——, 1978: Further evidence of traveling planetary waves. *J. Atmos. Sci.*, **35,** 1605–1618.

——, 1979: Observations of large-scale traveling Rossby waves. *Rev. Geophys. Space Phys.*, **17,** 1935–1949.

——, and K. Labitzke, 1981: A free Rossby wave in the troposphere and stratosphere during January 1979. *J. Geophys. Res.*, **86,** 1247–1254.

Pratt, R. W., and J. M. Wallace, 1976: Zonal propagation characteristics of large-scale fluctuations in the mid-latitude troposphere. *J. Atmos. Sci.*, **33,** 1184–1194.

Roads, J. O., and R. C. J. Somerville, 1982: Predictability of ultralong waves in global and hemispheric quasi-geostrophic barotropic models. *J. Atmos. Sci.*, **39,** 745–755.

Rossby, C. G., and collaborators, 1939: Relations between variations in the intensity of the zonal circulation of the atmosphere and the displacements of the semi-permanent centers of actions. *J. Mar. Res.*, **2,** 38–55.

Salby, M. L., 1980: The influence of realistic dissipation on planetary normal structures. *J. Atmos. Sci.*, **37,** 2186–2199.

——, 1981a: Rossby normal modes in nonuniform background configurations. Part I: Simple fields. *J. Atmos. Sci.*, **38,** 1803–1826.

——, 1981b: Rossby normal modes in nonuniform background configurations. Part II: Equinox and solstice conditions. *J. Atmos. Sci.*, **38,** 1827–1840.

Sommerville, R. C. J., 1980: Tropical influences on the predictability of ultralong waves. *J. Atmos. Sci.*, **37,** 1141–1156.

Straus, D. M., 1983: On the role of the seasonal cycle. *J. Atmos. Sci.*, **40,** 303–313.

——, and J. Shukla, 1981: Space–time spectral structure of a GLAS general circulation model and a comparison with observations. *J. Atmos. Sci.*, **38,** 902–917.